

Particle Tracking Microrheology of Complex Fluids

T. G. Mason,¹ K. Ganesan,² J. H. van Zanten,¹ D. Wirtz,¹ and S. C. Kuo²

¹*Department of Chemical Engineering, Johns Hopkins University, 221 Maryland Hall, 3400 North Charles Street, Baltimore, Maryland 21218*

²*Department of Biomedical Engineering, Johns Hopkins University, 720 Rutland Avenue, Baltimore, Maryland 21205*

(Received 21 January 1997; revised manuscript received 28 July 1997)

We present a new method for measuring the linear viscoelastic shear moduli of complex fluids. Using photodiode detection of laser light scattered from a thermally excited colloidal probe sphere, we track its trajectory and extract the moduli using a frequency-dependent Stokes-Einstein equation. Spectra obtained for polyethylene oxide in water are in excellent agreement with those found mechanically and using diffusing wave spectroscopy. Since only minute sample volumes are required, this method is well suited for biomaterials of high purity, as we demonstrate with a concentrated DNA solution. [S0031-9007(97)04234-8]

PACS numbers: 83.50.Fc, 83.70.Hq, 83.80.Lz, 83.85.Ei

Probing the rheological properties within cells is fundamentally important for understanding biological motility. However, the miniscule volume of cells precludes the use of standard mechanical and optical rheological techniques which require macroscopic sample volumes. Similarly, rheological measurements of purified biomaterials available only in small quantities have also been precluded. Microrheology, the study of the stress-strain relationship for small material volumes, may yield methods which overcome this volume limitation. Early studies have centered on video tracking the motion of colloidal magnetic beads driven by an applied magnetic field gradient [1,2]. However, the stresses driving the bead's motion may be large compared to those arising from thermal fluctuations; since many complex fluids and biomaterials are fragile with yield strains much smaller than unity, magnetic forcing may actually alter the local structure around the sphere so that nonlinear rheological properties are probed. Because of this problem, measuring the linear viscoelastic moduli of biological materials remains an important challenge.

Complex fluids contain extended polyatomic structures ranging from about one nanometer to several microns. These colloidal structures give rise to viscoelastic rheological behavior, in which energy is partially stored and dissipated within the material as it is perturbatively sheared. Many equivalent representations exist for quantifying an isotropic material's linear viscoelastic response; all can be ultimately recast in terms of a single scalar function of time, the stress relaxation modulus, $G_r(t)$, which has a magnitude set by the thermodynamic derivative of stress with respect to strain and relaxation time scales set by the decay of the stress autocorrelation function [3]. Complex Fourier transformation of $G_r(t)$ can be used to obtain the frequency-dependent complex shear modulus, $G^*(\omega)$, which has a real part, $G'(\omega)$, the elastic storage modulus, and an imaginary part, $G''(\omega)$, the viscous loss modulus [4]. Since both $G'(\omega)$ and $G''(\omega)$ arise from the single function $G_r(t)$, they are not independent functions but must obey the Kramers-Kronig relations.

In this Letter, we demonstrate that microscopic tracking of the thermally driven motion of a single particle suspended in a complex fluid can be used to measure the fluid's macroscopic linear viscoelasticity over an extended frequency range. By extracting the particle's time-dependent mean square displacement, $\langle \Delta r^2(t) \rangle$, from its trajectory measured using laser deflection particle tracking (LDPT), we obtain $G^*(\omega)$ from a frequency-dependent form of the Stokes-Einstein equation. This approach assumes that the shear stress relaxation in the locality of the particle is identical to that of the bulk fluid subjected to a perturbing shear strain and is valid when the length scales of heterogeneity of the discrete structures within the fluid are much smaller than the particle. To test this new approach, we compare particle-tracking measurements of $G^*(\omega)$ with corresponding mechanical and diffusing wave spectroscopy (DWS) measurements [5,6] for a model polymeric solution, and we find excellent agreement. As with DWS, single-particle tracking can be used to measure the viscoelastic moduli over an extended frequency range. However, LDPT requires a much smaller volume and can be used with complex fluids in which the aggregation of the probe spheres precludes a simple interpretation using DWS.

Our model fluid for testing LDPT is a semidilute solution of polyethylene oxide (PEO) with an average molecular weight of 5×10^6 at 3% by mass in water. The semidilute PEO solution forms a viscoelastic entanglement network with an average mesh size of $\xi \approx 1$ nm. Monodisperse polystyrene spheres of radii $a = 0.26 \mu\text{m}$ have been added at a volume fraction $\phi \approx 10^{-4}$ for LDPT; larger spheres having $a = 0.49 \mu\text{m}$ have been added at $\phi = 10^{-2}$ to ensure strong multiple scattering for DWS. LDPT requires only $5 \mu\text{l}$ sample volumes compared to $300 \mu\text{l}$ for DWS. All measurements have been made at temperature $T = 23^\circ\text{C}$ after an equilibration time of five days.

LDPT is a new light scattering microscopy technique which can detect the trajectory of a moving colloidal

sphere in two dimensions with Å-scale resolution. As with some optical tweezers [7], a laser beam ($\lambda = 670$ nm) is focused by the microscope's objective onto a sphere. However, by contrast to optical tweezers, we use low laser power (2 mW) so that the optical forces are small ($<5\%$) compared to the random entropic forces driving the sphere's motion in the solution. The forward scattered light is collected by a high numerical aperture [1.4 NA (numerical aperture)] condenser. If the sphere moves even slightly away from the beam's axis, the forward scattered light will contain an off-axis intensity asymmetry reflecting the sphere's position. This intensity asymmetry can be measured in two orthogonal directions by subtracting the photocurrent of opposing quadrant pairs of a photodiode detector centered about the optical axis beyond the condenser. The photocurrent differences are amplified and converted into voltages which yield the spatial coordinates of the sphere's center using a prior calibration of displacements generated by a piezoelectric x - y stage. (The voltage varies linearly for displacements out to 130 nm and exhibits a maximum at 200 nm.) The sphere's trajectory is obtained by sampling the voltages with a 12-bit A/D converter at rates up to 50 kHz. The spatiotemporal resolution is 0.01 nm/Hz $^{1/2}$ above 500 Hz, degrading to 1 nm/Hz $^{1/2}$ at 20 Hz due to mechanical resonances of the stage. To avoid wall effects, we consider a sphere at least 3 μ m away from the cover slip; the sphere is initially centered in the beam using feedback from the photodiode to control the x - y stage.

The trajectory of a sphere in the PEO solution measured using LDPT is shown in the inset of Fig. 1 over a duration

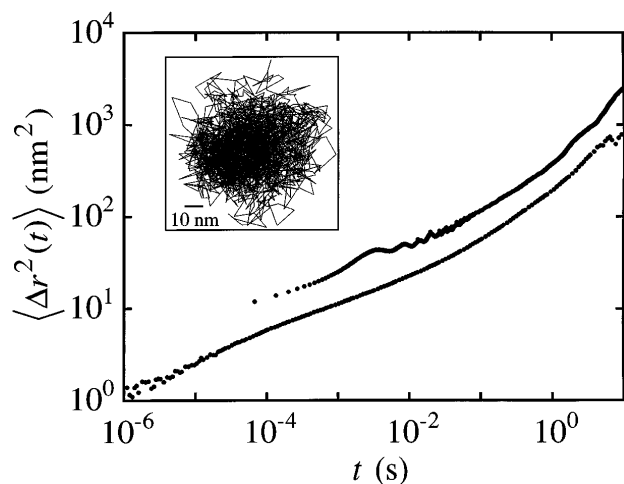


FIG. 1. The three-dimensional mean square displacement, $\langle \Delta r^2(t) \rangle$, as a function of time for polystyrene spheres in a viscoelastic entanglement network of polyethylene oxide (5×10^5 mol. wt.) at 3% by mass in water determined using LDPT (radius $a = 0.26$ μ m; upper curve) and DWS ($a = 0.49$ μ m; lower curve). Inset: two-dimensional trajectory measured using LDPT at a sampling rate of 15 kHz over 1 s.

of 1 s at a sampling rate of 15 kHz. The sphere remains in the linear voltage-displacement region at all times, and successive displacements are several orders of magnitude smaller than the sphere's size. This trajectory is much more compact than that for a sphere in water due to the elasticity of the polymer network. Using this trajectory, we calculate $\langle \Delta r^2(t) \rangle$ in two dimensions by sweeping the time lag and averaging over all possible initial times, assuming a stationary process [8]. We multiply this result by $3/2$ to obtain $\langle \Delta r^2(t) \rangle$ in three dimensions. To extend $\langle \Delta r^2(t) \rangle$ to longer times, a sampling rate of 150 Hz is also used; $\langle \Delta r^2(t) \rangle$ for both rates are shown in Fig. 1 (upper curve). The measured $\langle \Delta r^2(t) \rangle$ are reproducible to 10% standard deviation. Because of the entanglement elasticity of the PEO network, $\langle \Delta r^2(t) \rangle$ is subdiffusive at the earliest times, whereas at longer times, the slope on the log-log plot approaches unity, reflecting a terminal diffusive behavior due to the relaxation of entanglements. Mechanical vibrations of the stage introduce an oscillatory error in $\langle \Delta r^2(t) \rangle$ which is maximum at $t \approx 5 \times 10^{-3}$ s.

We have also measured $\langle \Delta r^2(t) \rangle$ using transmission DWS with a 2 mm thick rectangular cell. We illuminate the cell with an intensity-stabilized argon-ion laser in a single frequency mode at $\lambda = 514$ nm. The scattering mean free path of the light, $l^* = 166$ μ m [9], is much smaller than the cell thickness, ensuring strong multiple scattering from the spheres; scattering from the polymer is negligible by comparison. Correlation spectroscopy of the fluctuations of the scattered light intensity, caused by the motion of the spheres, is made using a digital correlator fed by a single-mode optical fiber and photomultiplier detection system. From the intensity correlation function, we calculate $\langle \Delta r^2(t) \rangle$ [9], as shown by the lower curve in Fig. 1. The shapes of the DWS and LDPT $\langle \Delta r^2(t) \rangle$ are in excellent agreement, and the LDPT $\langle \Delta r^2(t) \rangle$ lies nearly a factor of 2 above the DWS $\langle \Delta r^2(t) \rangle$, as expected for spheres with a differing by a factor of 1.9. The remaining error of about 10% may result from coupling of the sphere's axial motions to the transverse LDPT voltages.

Assuming that the complex fluid can be treated as an isotropic, incompressible continuum around a sphere, the fluid's viscoelastic spectrum, $\tilde{G}(s)$, can be calculated from the unilateral Laplace transform of $\langle \Delta r^2(t) \rangle$ using a generalized Stokes-Einstein equation [6],

$$\tilde{G}(s) = \frac{k_B T}{\pi a s \langle \Delta \tilde{r}^2(s) \rangle}, \quad (1)$$

where s is the Laplace frequency and k_B is Boltzmann's constant. Equation (1) is based on a generalized Langevin equation which describes the sphere's motion in the continuum (neglecting the sphere's inertia), and it is consistent with energy equipartition and the fluctuation-dissipation theorem. However, Eq. (1) is also based on the implicit assumption that Stokes drag for viscous fluids (no-slip boundary conditions) can be generalized to viscoelastic fluids at all s . Since this assumption may not

be true in general, Eq. (1) is phenomenological. From the measured $\langle \Delta r^2(t) \rangle$, we avoid the truncation errors introduced by taking the numerical Laplace transform, and instead estimate $\tilde{G}(s)$ by substituting $\langle \Delta r^2(t) \rangle$ into an algebraic Stokes-Einstein form,

$$\tilde{G}(s) \approx \frac{k_B T}{\pi a \langle \Delta r^2(t) \rangle \Gamma[1 + (\partial \ln \langle \Delta r^2(t) \rangle / \partial \ln t)]} \Big|_{t=1/s}, \quad (2)$$

where Γ is the gamma function. This form is physically justified since the slope of $\langle \Delta r^2(t) \rangle$ on a log-log plot must lie between zero and one, and the gamma function (which deviates from unity by at most 12%) is the conversion factor between transform pairs; it matches the numerical Laplace transform for s at which truncation errors are negligible. We calculate $G_r(t)$ by taking the inverse Laplace transform of $\tilde{G}(s)$ using the canonical method of relaxation spectra [4]; a fit of $\tilde{G}(s)$ to $\sum_j G_j s / (s + 1/\tau_j)$ (with τ_j chosen logarithmically to cover the desired range of s) is made using a nonlinear least squares routine, and $G_r(t)$ is reconstructed from a sum of decaying exponentials using weights, G_j , determined from the fit. The weights also determine the unilateral Fourier cosine and sine transforms of $G_r(t)$, which give $G'(\omega)$ and $G''(\omega)$, respectively [4]. This procedure provides an unbiased way to determine all relevant moduli from $\langle \Delta r^2(t) \rangle$.

We compute $\tilde{G}(s)$ from $\langle \Delta r^2(t) \rangle$ obtained using LDPT and DWS, as shown by the solid circles in Fig. 2; the $\tilde{G}(s)$ are nearly identical. By fitting $\tilde{G}(s)$, we calculate $|G^*(\omega)|$ (open circles) and $G_r(t)$ (inset). At the low ω , $|G^*(\omega)|$ rises with a slope of nearly unity; the terminal diffusive behavior in $\langle \Delta r^2(t) \rangle$ is equivalent to a low

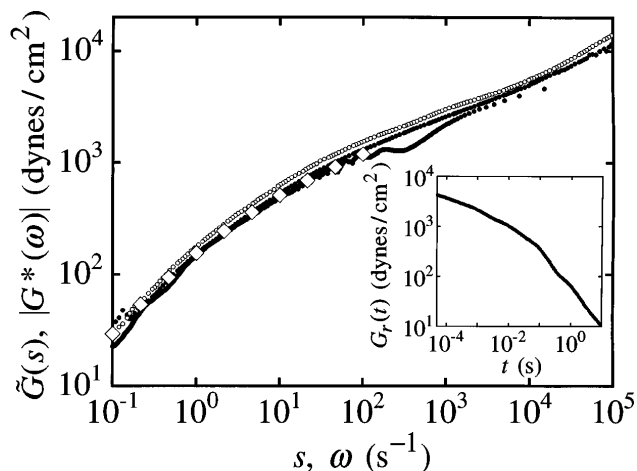


FIG. 2. Frequency-dependent magnitude of the viscoelastic spectrum, $\tilde{G}(s)$ (solid circles), for the 3% PEO solution determined from LDPT and DWS (lower and upper curves). Also plotted is the magnitude of the complex modulus, $|G^*(\omega)|$, from LDPT and DWS (open circles) and mechanical rheometry (large diamonds). Inset: the corresponding temporal dependence of the stress relaxation modulus, $G_r(t)$

frequency viscosity associated with the relaxation of colloidal entanglements. For larger ω , the slope becomes much less than one, reflecting a plateau elasticity of the network corresponding to the confinement region in $\langle \Delta r^2(t) \rangle$. At the highest ω , attained using DWS, the slope begins to rise toward unity again, reflecting the approach to an effective molecular viscosity of the water and polymer. We compare this $|G^*(\omega)|$ with that measured for the pure PEO solution using a controlled-strain rheometer with a cone and plate geometry (sample volume of 0.2 ml) at a strain of $\gamma = 0.02$ in the linear regime. The mechanical $|G^*(\omega)|$ confirm those found from LDPT and DWS.

Having demonstrated the validity of our approach for a PEO network, we apply it to concentrated DNA in a saline buffer. We disperse linear, double-stranded DNA from calf thymus having an average number $N = 1.3 \times 10^4$ base pairs at $C_{\text{DNA}} = 10$ mg/ml in an aqueous buffer containing [tris-HCl] (pH 7.9) = 10 mM, [NaCl] = 50 mM, [KCl] = 50 mM, [MgCl₂] = 5 mM, [BSA] = 15 $\mu\text{g/ml}$, and [EDTA] = 0.1 mM. (BSA is bovine serum albumin, and EDTA is ethylene diaminetetra-acetic acid.) These DNA are available in sufficient quantity to permit mechanical measurements. Agitation over one week renders the solution homogeneous. Even at $\phi \approx 0.01$, microscopy reveals aggregation of the spheres. This aggregation precludes the use of DWS to determine $G^*(\omega)$, since DWS averages over the motion of all particles, including those surrounded by neighbors within the aggregate; this motion is not the same as that for an isolated particle in the DNA solution, so Eq. (1) cannot be used. However, since LDPT works at effectively zero ϕ , this problem is eliminated, and $G^*(\omega)$ can be measured.

A comparison of $G'(\omega)$ and $G''(\omega)$ for concentrated DNA measured mechanically (solid and open diamonds) and using LDPT (solid and dashed lines) with piezoelectric calibration setting the magnitude is shown in Fig. 3. The two methods agree remarkably well; moreover, LDPT extends two decades higher in ω . The concentrated DNA exhibits classical features of polymer entanglement networks, including a plateau elasticity at high ω and a low frequency viscous relaxation of entanglements at low ω .

The feasibility of using LDPT to determine macroscopic viscoelasticity hinges upon several assumptions. The good agreement we find for the PEO entanglement network is strong evidence that the local moduli surrounding the particle are identical to the bulk moduli; this continuum assumption underlying Eq. (1) holds as expected for $\xi \ll a$, but it may break down for $a\xi$. Our observations also directly show that the PEO entanglement network is an ergodic material, since $\langle \Delta r^2(t) \rangle$ determined by ensemble averaging over many probe spheres (DWS) is equivalent to $\langle \Delta r^2(t) \rangle$ determined by time averaging over the motion of a single isolated sphere assuming a stationary process (LDPT). This equivalence is implied

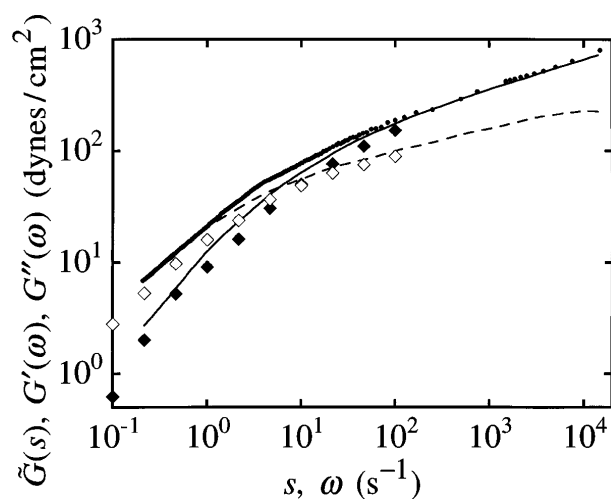


FIG. 3. Frequency dependence of the storage and loss moduli, $G'(\omega)$ and $G''(\omega)$, for DNA (1.3×10^4 kbp) at 10 mg/ml in an aqueous saline buffer measured using LDPT (solid and dashed lines) and mechanically (solid and open diamonds). The measured viscoelastic spectrum, $\tilde{G}(s)$, from LDPT is coplotted as the solid circles.

since the measured $|G^*(\omega)| \rightarrow 0$ as $\omega \rightarrow 0$. By contrast, for nonergodic materials, such as glasses which can have structural modes of relaxation related to length scales much greater than a , these two averages are not equivalent, and it may be necessary to track many particles at different localities within the material to build a true ensemble-averaged $\langle \Delta r^2(t) \rangle$ from which the moduli can be extracted.

In addition to LDPT, we have used video particle tracking (VPT) [10] as a complementary technique and obtained good agreement with all other methods. For weak materials in which the particle may diffuse quickly out of the linear voltage-distance range of LDPT, VPT is more appropriate. According to Eq. (1) and the nanometer-scale spatial resolution, VPT is limited to $|G^*(\omega)| \leq 10^3$ dyn/cm² and frequencies less than 15 Hz for micron-sized spheres, whereas we project that LDPT can be used to measure extremely elastic complex fluids with $|G^*(\omega)| \leq 10^7$ dyn/cm², due to its higher spatial resolution.

Since particles can be tracked in many ways, we envision numerous extensions of the essential microrheologi-

cal method we have presented. Faster video hardware may be used to increase the frequency range of VPT, and faster A/D sampling may allow LDPT to reach the megahertz range, rivalling DWS. Interferometric particle-tracking methods [11] may also be used to attain similarly high resolution, albeit only in a single dimension. Confocal microscopy may permit full real-space visualization of the trajectory. By detecting $\langle \Delta r^2(t) \rangle$ along independent directions, it may be possible to measure the anisotropic viscoelastic moduli of materials having oriented microstructures. Ultimately, the tracking of organelle motion inside cells using the principles we have outlined may yield a completely noninvasive method for *in vivo* microrheology.

We thank K. Rufener for his help with the DWS measurement. D.W. thanks the National Science Foundation (DMR 9623972) and the Whitaker Foundation for financial support.

-
- [1] F. Ziemann, J. Rädler, and E. Sackmann, *Biophys. J.* **66**, 2210 (1994).
 - [2] F. Amblard, A.C. Maggs, B. Yurke, A.N. Pargellis, and S. Leibler, *Phys. Rev. Lett.* **77**, 4470 (1996).
 - [3] J.-P. Hansen and I.R. McDonald, *Theory of Simple Liquids* (Academic, London, 1986).
 - [4] R.B. Bird, R.C. Armstrong, and O. Hassager, *Dynamics of Polymeric Liquids* (John Wiley and Sons, New York, 1977).
 - [5] T.G. Mason, H. Gang, and D.A. Weitz, *J. Opt. Soc. Am. A* **14**, 139 (1997).
 - [6] T.G. Mason and D.A. Weitz, *Phys. Rev. Lett.* **74**, 1250 (1995).
 - [7] S.B. Smith, Y. Cui, and C. Bustamante, *Science* **271**, 795 (1996).
 - [8] F. Reif, *Fundamentals of Statistical and Thermal Physics* (McGraw-Hill, New York, 1965).
 - [9] D.A. Weitz and D.J. Pine, in *Dynamic Light Scattering*, edited by W. Brown (Oxford University Press, Oxford, 1992).
 - [10] S.C. Kuo, J. Gelles, E. Steuer, and M.P. Sheetz, *J. Cell Sci. Suppl.* **14**, 135 (1991).
 - [11] K. Svoboda, C.F. Schmidt, B.J. Schnapp, and S.M. Block, *Nature (London)* **365**, 721 (1993).